Effect of Microchannel Aspect Ratio on Residence Time Distributions and the Axial Dispersion Coefficient

J. Aubin*, L. Prat, C. Xuereb, C. Gourdon
Laboratoire de Génie Chimique CNRS / INPT / UPS, University of Toulouse, France

*Correspondence:

Dr. Joëlle Aubin Laboratoire de Génie Chimique CNRS / INPT / UPS, University of Toulouse, 6 allée Emile Monso BP-34038, 31029 Toulouse Cedex 4, France
Email : joelle.aubincano@ensiacet.fr
Tel : +33 534 615 243 Fax : +33 534 615 253

Abstract

The effect of microchannel aspect ratio (channel depth/channel width) on residence time distributions and the axial dispersion coefficient have been investigated for Newtonian and shear thinning non-Newtonian flow using computational fluid dynamics. The results reveal that for a fixed cross sectional area and throughput, there is a narrowing of the residence time distribution as the aspect ratio decreases. This is quantified by an axial dispersion coefficient that increases rapidly for aspect ratios less than 0.3 and then tends towards an asymptote as the aspect ratio goes to 1. The results also show that the axial dispersion coefficient is related linearly to the Reynolds number when either the aspect ratio or the mean fluid velocity is varied. However, the fluid Péclet number is a linear function of the Reynolds number only when the aspect ratio (and therefore hydraulic diameter) is varied. Globally, the results indicate that microchannels should be designed with low aspect ratios (≤ 0.3) for reduced axial dispersion.

Keywords. *residence time distributions (RTD; axial dispersion; aspect ratio; microchannel; microreactor; computational fluid dynamics (CFD); laminar flow.*

1 Introduction

Amongst the different criteria used for characterising the performance of microreactors, the determination of residence time distributions is particularly important when chemical reaction applications are considered. Due to the predominantly laminar flow in microreactors, the velocity profile in the microchannel is typically parabolic; this gives rise to temporal inhomogeneities in the flow, which translates into wide residence time distributions. For chemical reaction applications, the broadening of the residence time distribution most often results in a decrease of the selectivity for the desired product and/or of the product quality. For this reason, a number of studies in the chemical engineering literature have been devoted to the experimental [1-7] or numerical [8-12] determination of residence time distributions and associated modelling. Most of these studies deal with the performance evaluation of existing or new microreactor geometries and the comparison of different designs in terms of residence time distributions. On the other hand, little attention has been paid to basic channel design in microreactors and microstructured reactors, and the effects on residence time distribution.

In the design of microchannels within microreactors, the basic geometrical parameters are often conditioned by the microfabrication techniques available for the microchannel manufacturing. Today, many techniques lead to the fabrication of microchannels with a rectangular cross section. The different geometrical parameters of such microchannels are few: the channel depth, width and length, as well as the topographical shape. It has previously

been shown that the topographical shape of the microchannels can influence the performance of both single and two-phase flow applications. In particular, meandering channels give rise to secondary flow patterns and in some cases Dean vortices, which reduce the broadening of residence time distributions, improve mixing and enhance heat transfer significantly (e.g. [2, 4, 8, 13, 14]). In contrast, the effects of the channel dimensions and the associated aspect ratio, α (channel depth/channel width), on transport phenomena are less detailed. It is well known that for laminar flow in macro-scale rectangular ducts the aspect ratio affects the friction factor f (and therefore the pressure drop), as well as heat transfer [15]. For fully developed laminar flow, the product f Re decreases towards an asymptotic limit as the aspect ratio approaches unity. In heat transfer applications, the aspect ratio modifies the Nusselt number, depending on the number and disposition of the walls transferring heat. These trends can be expected to be the same for flow in sub-millimeter channels. On the other hand, some specific studies on the effects of aspect ratio on mixing and diffusion in microchannels have been conducted. Gobby et al. [16] investigated the effects of aspect ratio on mixing of gases in T-micromixers using computational fluid dynamics (CFD). They modified the aspect ratio in two ways: by keeping the microchannel width constant and then the hydraulic diameter constant. At constant width, the channel length required for mixing was almost independent of the aspect ratio, whereas for constant hydraulic diameter, the mixing length decreased for increasing aspect ratio (and hence decreasing channel width). This is logical since the characteristic length for diffusion decreases and the interface between fluids increases. Chen et al. [17] studied the effect of aspect ratio in the range of 0.05–1 (with constant channel

width) on diffusive liquid mixing in a T-micromixer. They found that non-uniform mixing by diffusion (the butterfly effect) originates from the top and bottom microchannel walls and is more pronounced for aspect ratios > 0.5. However, no recommendations on best channel design were made. Finally, Dutta et al. [18, 19] have investigated the effect of aspect ratio on Taylor-Aris dispersivity in microchannels. In long-time dispersion regimes, i.e. where the characteristic fluid processing time is equivalent to or greater than the time for molecular diffusion (Fourier number, Fo ≥ 1), the axial (convective) dispersion in laminar flows is limited by molecular diffusion across the streamlines. Taylor [20] described this process by an effective dispersivity, which is linearly dependent on the square of the Peclet number, with a slope that is a function of the shape of the channel cross section. Dutta et al. [18, 19] determined the geometrical coefficient that relates the square of the Peclet number to the effective dispersivity for various channel aspect ratios of rectangular microchannels. For a fixed channel depth, the authors found that as the aspect ratio increased in the limit of $\alpha \rightarrow 1$ (reducing the cross sectional area), the coefficient decreased. On the other hand, for a fixed cross sectional area the coefficient increased asymptotically as the aspect ratio increased in the limit of $\alpha \rightarrow 1$. For the microfluidic applications considered by those authors (for example chromatographic separations), it is suggested that microchannels be designed by choosing the smallest possible microchannel depth that can be fabricated and then the appropriate aspect ratio to achieve the desired flow rate; this will result in limited Taylor-Aris dispersion.

In this work, the effect of microchannel aspect ratio on residence time distribution and the axial dispersion coefficient obtained with both Newtonian and shear-thinning fluids is

investigated. It employs a chemical engineering approach focussing on the use of microreactors and microstructured reactors for production purposes. In this respect, the aim is to gain insight on how to design rectangular channels for a desired throughput and how axial dispersion is modified with the aspect ratio and typical dimensionsless numbers. The approach described in this study employs CFD to compute the velocity fields and Lagrangian particle tracking for determining residence time distributions. Moreover, it is a generalised methodology that can be applied to flows in all types of reactor geometries and with rheologically complex fluids.

2 Microchannel Geometries

Rectangular microchannels of length L = 0.005 m have been used in this study. The channel aspect ratio is defined as α = channel depth (H) / channel width (W) and has been varied from 0.05–1 whilst keeping a constant channel cross-sectional area of A = 2.25×10^{-8} m^2. The aspect ratios and the corresponding channel dimensions, including the hydraulic diameter (defined as d_H = 4A / wetted perimeter) are given in Table 1. The L / d_H ratio then varies from 33–78 as the aspect ratio decreases. The residence times distributions obtained in the rectangular channels are compared with that obtained in a tubular microchannel with radius r ≈ 85 μm, giving a cross-sectional area equal to A.

3 Numerical Methods

The numerical simulation of the flow in the microchannels has been performed using ANSYS-CFX11 [21]. This is a general purpose commercial CFD package that solves the Navier-Stokes equations using a finite volume method via a coupled solver. The analysis procedure has been carried out in two steps. Firstly, the velocity and pressure fields in the mixer are solved. These values are then used to calculate particle trajectories within the flow field, which are used to determine the residence time distributions.

3.1 Flow computation

For each microchannel geometry, a mesh with an inflation layer on the channel walls was created, as shown in Figure 1. The mesh for each microchannel comprised approximately 550 000 prismatic and hexahedral elements (400 000 nodes). A preliminary grid convergence study was carried out in order to verify that the solution is grid independent. Water (μ = 0.00089 Pa.s, ρ = 997 kg.m^{-3}) was used as the principal Newtonian fluid; other model Newtonian fluids with viscosities of 0.02, 0.05 and 0.1 Pa.s were also tested. The non-Newtonian fluid was a 0.5 % Sodium Carboxymethyl Cellulose (CMC) solution (n = 0.3896, K = 2.904 Pa.s^n, μ_0 = 0.21488 Pa.s), which exhibits shear thinning behaviour. To describe this behaviour, a modified power law model [22] was used.

$$\mu_a = \frac{\mu_0}{1 + \frac{\mu_0}{K}\dot{\gamma}^{1-n}} \qquad (1)$$

where K is the consistency index and n is the flow behaviour index, which is equal to 1 for a Newtonian fluid. This model takes into account the Newtonian behaviour exhibited by shear thinning fluids at low shear rates, the power law behaviour at high shear rates and an a transitional regime at intermediate shear rates. The associated Reynolds number is the modified power law fluid Reynolds number, Re_m for flow in rectangular ducts as described by Park and Lee [23].

The boundary condition at the channel inlet was described by a laminar velocity profile for rectangular ducts using the approximation given in Shah and London [15]. This ensures that the fully developed laminar velocity profile is reached very quickly. In order to investigate the effects of the microchannel aspect ratio for both the Newtonian and shear thining fluids, and also Newtonian viscosity, the mean velocity, u, was fixed at 0.01 ms^{-1} for all channel geometries; this enabled their comparison at constant throughput. This corresponds to a laminar flow regime with Reynolds numbers (Re) in the range 0.014–1.68 for the Newtonian fluids and Re_m = 0.008–0.014 for the shear thinning fluid, depending on the aspect ratio of the microchannel. To investigate the effect of velocity on axial dispersion, a range of mean velocities were simulated in a single geometry (α = 1) corresponding to corresponding Reynolds number ranges of 0.4–2 and 0.006–0.03 for the Newtonian and power law fluids, respectively. At the outlet, a constant pressure condition (P = 1 atm) was

imposed and no-slip boundary conditions were applied at all walls. The ANSYS-CFX11 solver was used to solve the steady-state momentum and continuity equations for the fluid flow in the microchannels. The advection terms in each equation were discretized using a bounded second order differencing scheme to minimise the effects of numerical diffusion. Simulations were typically considered converged when the normalised residuals for the velocities fell below 1×10^{-6}.

3.2 Particle tracking

In this study, massless fluid particles are followed using a Lagrangian particle tracking method in order to determine the residence time distributions. This approach avoids the introduction of numerical diffusion that results if a scalar is tracked, which confuses the mixing behaviour. In addition to the fact that no interaction between the individual particles exists, it must be pointed out that this method does not take into account species transport by molecular diffusion. This is a valid assumption in the cases studied here since the process time, i.e. the mean residence time, of the fluid in the microchannels is much shorter than the time needed to mix radially by molecular diffusion and therefore Taylor-Aris dispersion is negligible.

Once the velocity field has been computed, 5000 weightless particles that are randomly distributed over the section of the microchannel inlet are released into the flow. The

movement of the particle tracers in the flow is then determined by integrating the vector equation of motion for each particle:

$$\frac{\mathrm{d}\mathbf{x}}{\mathrm{d}\,\mathrm{t}} = u(\mathbf{x}) \qquad (2)$$

In order to obtain a sufficient degree of accuracy when integrating the equation of motion, a fourth order Runge-Kutta scheme with adaptive step size has been employed. Furthermore, a restitution coefficient of unity is applied to the microchannel walls. This avoids particle trajectories being trapped near the walls where the local velocity is close to zero (less than 2 % of particles are stopped between the inlet and the outlet of the mixer).

3.3 Residence time distribution

The RTD for the fluid flowing through the various microchannel geometries was calculated by determining the particle trajectories as described in paragraph 3.2, and by recording the particle residence times from 1 mm after the inlet to the outlet of the microchannel. By recording the residence times after 1 mm of channel length, a fully developed laminar flow is ensured since 1 mm is 10-25 times longer than a typical laminar flow development length, estimated for a uniform velocity profile at the channel inlet. This is particularly important for non-Newtonian flows whose velocity profiles are not accurately approximated by the rectangular channel velocity profile approximation given in [15]. The residence time distribution, E(t), as described by Fogler [24], can then computed as:

$$E(t) = \frac{\Delta N_w}{N_w} \cdot \frac{1}{\Delta t} \qquad (3)$$

where ΔN_w is the number of particles that have a residence time in the mixer between time t and t+Δt each weighted by their initial velocity normalised by the maximum velocity in the microchannel and N_w is the total weight number of particles released in the microchannel. This approach is equivalent to the analysis of a pulse injection of tracer. From E(t), the first and second moments, i.e. the mean residence time, t_m, and the variance about the mean, σ^2, as well as a normalised residence time distribution, $E^*(t)$, can be determined. For open systems the mean residence time and the variance are related to the reactor Péclet number Pe_r [24], following:

$$\frac{\sigma^2}{t_m^2} = \frac{2}{Pe_r} + \frac{8}{Pe_r^2} \qquad (4)$$

The reactor Péclet number is defined as:

$$Pe_r = \frac{uL}{D_a} \qquad (5)$$

where L is the characteristic length defined by the length of the channel and D_a is the axial dispersion coefficient. Relation (4) is derived from the 1-dimensional axial dispersion model in which D_a is defined as the resultant of three components being molecular diffusion, turbulent diffusion and spatial dispersion [25]:

$$D_a = D_m + D_t + D_s \quad (6)$$

For the cases considered in the present study, molecular diffusion is considered negligible and the turbulent diffusion is null. As a result, the axial dispersion is entirely due to spatial dispersion, which is induced by the heterogeneities in the laminar velocity profile.

4 Results & Discussion

Residence time distributions are important for evaluating the performance of chemical reactors and are of particular relevance to the performance of microreactors, where the flow is typically laminar and there is much axial dispersion. Figure 2 shows the normalised residence time distributions for the laminar flow of a Newtonian fluid in rectangular microchannels with different aspect ratios and compares them with that obtained in a tubular microchannel with an equivalent cross-section. Firstly, it is clear that there is a relatively large amount of dispersion for all represented cases, which is not surprising for laminar flow. The microchannel with a square cross section ($\alpha = 1$) results in more axial dispersion than a tubular microchannel, whilst the RTD in the microchannel with $\alpha = 0.5$ is equivalent to that obtained with the circular cross-section. As the aspect ratio decreases and the microchannels become wide and shallow, the spread of the RTD curves decreases and shifts towards that of an ideal plug flow. In fact, as the aspect ratio decreases the centreline velocity across the width of the channel flattens out and the maximum velocity decreases. As a result, the velocity distribution in the channel cross section narrows, decreasing the standard deviation about the mean velocity.

Figure 3 shows the effect of microchannel aspect ratio on the RTD obtained with the non-Newtonian shear thinning fluid and compares the RTD for $\alpha = 1$ with the results of the Newtonian fluid. It can be seen that as the flow behaviour index passes from $n = 1$ for the Newtonian fluid to $n = 0.39$ for the power law fluid, there is a decrease in the spread of the RTD and a shift towards plug flow. This agrees with the numerical and experimental observations made by other authors for shear-thinning pseudoplastic flows in coiled tubes [26-28] and corresponds to a flattening of the axial velocity profile, which subsequently decreases the axial dispersion. As the aspect ratio decreases, the RTD curves of the non-Newtonian fluid narrow and approach that of ideal plug flow, in a similar manner to that observed for the Newtonian fluid.

The observations made from the RTD in Figures 2 and 3 can be quantified via the Péclet number which is related to the moments of the residence time distribution by equation (4). Figure 4 presents the reactor Péclet number as a function of the microchannel aspect ratio for both the Newtionian and power law fluids. As a higher Péclet number indicates smaller axial dispersion, the graph quantifies the reduction in axial dispersion when using the model non-Newtonian fluid compared with the Newtonian fluid. Furthermore, it clearly shows that the Péclet number decreases towards an asymptotic value as the aspect ratio increases and approaches a value of 1. Hence, axial dispersion is reduced with decreasing aspect ratio, i.e. as the channels become wide and shallow. It can be seen that as the aspect ratio decreases below approximately $\alpha = 0.3$, the changes in the Péclet number become increasingly important, reducing thus the axial dispersion at the same rate. It is interesting to note that the

shapes of the curves given in Figure 4 are very similar to that given by Shah and London [15] for the symmetric wall heating of macro scale rectangular ducts. They present the Nusselt number as a function of the aspect ratio and show that the Nusselt number increases (and therefore convective heat transfer) as the ducts become wide and shallow. Furthermore, the tangents to their curve at $\alpha = 0$ and $\alpha = 1$ intersect at approximately $\alpha \approx 0.3$; it is at values of α below this that convective heat transfer is rapidly improved.

From the Péclet number, one can deduce the axial dispersion coefficient. Figure 5 presents the effect of the aspect ratio on the axial dispersion coefficient. As expected, the values of the dispersion coefficients are lower for the modified power law fluid than for the Newtonian fluid and they increase asymptotically as $\alpha \to 1$. Quantitatively, the values of the axial dispersion coefficients are of the order of 10^{-6} m.s^{-2}, which is approximately 1000 faster than molecular diffusion in liquids.

When the aspect ratio of a channel decreases for a given cross-sectional area, the hydraulic diameter also decreases, which results of course in a decrease of the Reynolds number. In Figure 6, the effects of varying different parameters of the Reynolds number on the axial dispersion coefficient are considered for both the Newtonian and the non-Newtonian fluids. The Reynolds number is modified in one of three ways: by varying the aspect ratio – and therefore the hydraulic diameter – at fixed flowrate (i.e. mean velocity); by varying the flowrate at fixed aspect ratio; by varying the viscosity whilst keeping the flowrate and aspect ratio constant. It can be seen that the axial dispersion coefficient is linearly dependent on the

Reynolds number when either the flowrate (or mean velocity) or the aspect ratio are varied, and the importance of both parameters appear to be similar. On the other hand, the axial dispersion coefficient is independent of the Reynolds number when the Reynolds number is modified by the Newtonian fluid viscosity.

An alternate manner of presenting the data in Figure 6 is adimensionally. Figure 7 presents the fluid Péclet number as a function of the Reynolds number, the latter being varied by modifying the aspect ratio, the mean velocity or the fluid viscosity. Using this representation, it can be seen that there is a linear dependence of the Péclet number on the Reynolds number only if the Reynolds number is modified by varying the aspect ratio (or hydraulic diameter) of the microchannel. The Péclet number remains more or less constant over the range of Reynolds numbers studied when the mean velocity or the Newtonian viscosity of the fluids is modified.

5 Conclusions

CFD simulations of Newtonian and shear thinning fluid flows have been performed in order to evaluate the effect of microchannel aspect ratio on residence time distribution and axial dispersion. The approach described for calculating the residence time distributions is a generalised methodology that can be applied to all types of reactor geometries and complex fluids. For straight channels where the streamlines are linear and parallel to the main axis, residence time distributions can essentially be estimated from the fully developed laminar

velocity profile. However, for arbitrary channel cross sections and non-Newtonian flows, the laminar velocity profiles cannot be approximated by simple equations. The advantage of using CFD to resolve the Navier-Stokes equations is that the fully developed laminar velocity profile and fields can be determined for a given geometry and fluid type (in the limits of the fluid model). Furthermore, the use of Lagrangian particle tracking enables the residence times of massless tracer elements to be determined, which is particularly important when the particle trajectories are not linear, such as in complex reactor geometries.

In this study, it has been shown that for constant cross sectional area and constant throughput, the residence time distributions narrow as the aspect ratio decreases. This effect is found to be even more pronounced for the shear thinning non-Newtonian flow. The residence time distributions are quantified by the reactor Péclet number, which is shown to decrease asymptotically as the aspect ratio increases. The Péclet number starts to increase sharply at aspect ratios approximately < 0.3, signifying reduction in axial dispersion. The axial dispersion coefficient has shown to increase asymptotically with increasing aspect ratio and is linearly dependent on the Reynolds number if the latter is varied by the velocity or the aspect ratio. On the other hand, the fluid Péclet scales with the Reynolds number only if the channel aspect ratio is varied.

Overall, the results of this study indicate that in order to obtain narrowed residence time distributions and reduced axial dispersion, microchannels should be designed with low aspect ratios (approximately $\alpha \leq 0.3$) such that the channels are wide and shallow. The same

range of aspect ratios has also shown to be favourable for uniform diffusive mixing [17] and improved convective heat transfer [15].

Acknowledgements This work was funded by the Integrated Project IMPULSE (project no. NMP2-CT-2005-011816), www.impulse-project.net, within the 6th Framework Programme of the European Commission.

List of symbols

d_H hydraulic diameter (4HW/(2(H+W)) [m]

D_a axial dispersion coefficient [$m.s^{-2}$]

D_m molecular diffusion coefficient [$m.s^{-2}$]

D_s spatial dispersion coefficient [$m.s^{-2}$]

D_t turbulent diffusion coefficient [$m.s^{-2}$]

E(t) residence time distribution function [–]

E*(t) normalised residence time distribution function ($E(t).t_m^{-1}$) [–]

f friction factor [–]

H depth of microchannel [m]

K power law consistency [$Pa.s^n$]

l characteristic length scale [m]

L microchannel length [m]

n power law flow index [–]

N_w total weighted number of tracer particles [–]

ΔN_w velocity weighted number of tracer particles exiting the microchannel in a given time class [–]

P pressure (Pa)

t time [s]

t_m mean residence time [s]

u mean velocity [$m.s^{-1}$]

W width of microchannel [m]

Greek letters

α aspect ratio (H/W) [–]

β shear rate parameter $((\mu_0/K).(u/d_H)^{1-n})$ [–]

$\dot{\gamma}$ shear rate [s^{-1}]

μ Newtonian viscosity [Pa.s]

μ_0 zero shear rate viscosity [Pa.s]

μ_a apparent viscosity [Pa.s]

μ^* reference viscosity $(\mu_0.(1+\beta)^{-1})$ [Pa.s]

ρ density [$kg.m^{-3}$]

σ^2 variance about the mean residence time [s^2]

Dimensionless numbers

Fo Fourier ($tD_m.l^{-2}$)

Pe_r Reactor Péclet number ($uL.D_a^{-1}$)

Pe_f Fluid Péclet number ($ud_H.D_a^{-1}$)

Re Reynolds number ($\rho\, ud_H.\mu^{-1}$)

Re_g Generalised power law fluid Reynolds number ($\rho\, u^{2-n}d_H^{\,n}.K^{-1}$)

Re_m Modified power law fluid Reynolds number ($\rho\, ud_H.\mu^{*-1}$)

Sc Schmidt number ($\mu.(\rho\, D_m)^{-1}$)

References

[1] M. Günther, S. Schneider, J. Wagner, R. Gorges, Th. Henkel, M. Kielpinski, J. Albert, R. Bierbaum, J.M. Köhler, Characterisation of residence time and residence time distribution in chip reactors with modular arrangements by integrated optical detection, *Chem. Eng. J.* 101 (2004) 373-378

[2] A. Günther, S.A. Khan, M. Thalmann, F. Trachsel, K.F. Jensen, Transport and reaction in microscale segmented gas-liquid flow, *Lab Chip* , (2004) 278-286

[3] K. Golbig, A. Kursawe, M. Hohmann, S. Taghavi-Moghadam, T. Schwalbe, Designing Microreactors in Chemical Synthesis – Residence-time Distribution of Microchannel Devices, *Chem. Eng. Comm*. 192 (2005) 620-629

[4] F. Trachsel, A. Günther, S. Khan, K.F. Jensen, Measurement of residence time distribution in microfluidic systems, *Chem. Eng. Sci*. 60 (2005) 5729-5737

[5] W. Salman, P. Angeli, A. Gavriilidis, Sample Pulse Broadening in Taylor Flow Microchannels for Screeing Applications, *Chem. Eng. Technol*. 28 (2005) 509-514

[6] J.-M. Commenge, T. Obein, G. Genin, X. Framboisier, S. Rode, V. Schanen, P. Pitiot, M. Matlosz, Gas-phase residence time distribution in a falling-film microreactor, *Chem. Eng. Sci*. 61 (2006) 597-604

[7] D. Boskovic, S. Loebbecke, Modelling of the residence time distribution in micromixers, *Chem. Eng. J*. 135S (2008) S138-S146

[8] F. Jiang, K.S. Drese, S. Hardt, M. Küpper, F. Schönfeld, Helical Flows and Chaotic Mixing in Curved Microchannels, *AIChE J*. 50 (2004) 2297-2305

[9] J. Aubin, D.F. Fletcher, C. Xuereb, Design of micromixers using CFD modelling, *Chem. Eng. Sci*. 60 (2005) 2503-2516

[10] J.T. Adeosun, A. Lawal, Mass transfer enhancement in microchannel reactors by reorientation of fluid interfaces and stretching, *Sens. Actuators B* 110 (2005) 101-111

[11] W. Salman, A. Gavriilidis, P. Angeli, Axial Mass Transfer in Taylor Flow through Circular Microchannels, AIChE J., 53 (2007) 1413-1428.

[12] C. Amador, D. Wenn, J. Shaw, A. Gavriilidis, P. Angeli, Design o a mesh microreactor for even flow distribution and narrow residence time distribution, *Chem. Eng. J*. 135S (2008) S259-S269

[13] P.E. Geyer, N.R. Rosaguti, D.F. Fletcher, B.S. Haynes, Thermohydraulics of square-section microchannels following a serpentine path, *Microfluid Nanofluid* 2 (2006) 195-204

[14] F. Sarrazin, L. Prat,, N. Di Miceli, G. Cristobal, D.R. Link, D.A.Weitz, Mixing characterization of microdroplets engineering on a microcoalescer, Chem. Eng. Sci. 62 (2007) 1042-1048

[15] R.K. Shah and A.L. London, *Laminar Flow Forced Convection in Ducts*, Academic Press Inc., NY (1978)

[16] D. Gobby, P. Angeli, A. Gavriilidis, Mixing characteristics of T-type microfluidic mixers, *J. Micromech. Microeng*. 11 (2001) 126-132

[17] J.M. Chen, T.-L. Horng, W.Y. Tan, Analysis and measurements of mixing in pressure-driven microchannel flow, *Microfluid Nanofluid* 2 (2006) 455-469

[18] D. Dutta, D.T. Leighton Jr., Dispersion Reduction in Pressure-Driven Flow Through Microetched Channels, *Anal. Chem*. 73 (2001), 504-513

[19] D. Dutta, A. Ramachandran, D.T. Leighton Jr., Effect of channel geometry on solute dispersion in pressure-driven microfluidic systems, *Microfluid Nanofluid* 2 (2006) 275-290

[20] G.I. Taylor, Dispersion of soluble matter in solvent flowing slowly through a tube, *Proc. R. Soc. (London)* 219A (1953) 186-203

[21] ANSYS (2007) www.ansys.com/cfx

[22] J.E. Dunleavy and S. Middleman, Relation of shear behavior of solutions of polyisobutylene, *Trans Soc Rheol* 10 (1966) 151

[23] S. Park, D.-R. Lee, Experimental and numerical investigations of pressure drop in a rectangular duct with modified power law fluids, *Heat Mass Transfer* 39 (2003) 645-655

[24] H.S. Fogler, *Elements of Chemical Reaction Engineering*, 2nd Ed., PTR Prentice Hall, Englewood Cliffs NJ, (1992)

[25] J.-P. Couderc, C. Gourdon, A. Liné, *Phénomènes de transfert en génie des procédés*, Lavoisier Paris (2008) 230-232.

[26] V.R. Ranade and J.J. Ulbrecht, Velocity profiles of Newtonian and non-Newtonian toroidal flows measured by a LDA technique, *Chem. Eng. Commun.* 20 (1982) 253-272.

[27] A.K. Saxena, K.M. Nigam, K.P.D. Nigam, RTD for diffusion-free laminar flow of non-Newtonian fluds through coiled tubes, *Can. J. Chem. Eng*. 61 (1983) 50-52.

[28] C. Castelain and P. Legentilhomme, Residence time distribution of a purely viscous non-Newtonian fluid in helically coiled of spatially chaotic flows, *Chem. Eng. J.* 120 (2006) 181-191.

Table 1 Channel aspect ratio, α, and corresponding channel dimensions.

α = H / W	H (µm)	W (µm)	d_H (µm)
1 / 20	33	671	64
1 / 10	47	474	86
1 / 8	53	424	94
1 / 6	61	367	105
1 / 4	75	300	120
1 / 2	106	212	141
1	150	150	150

List of Figures

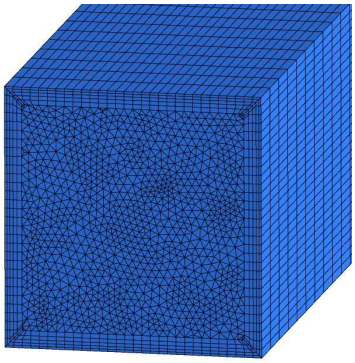

(a)

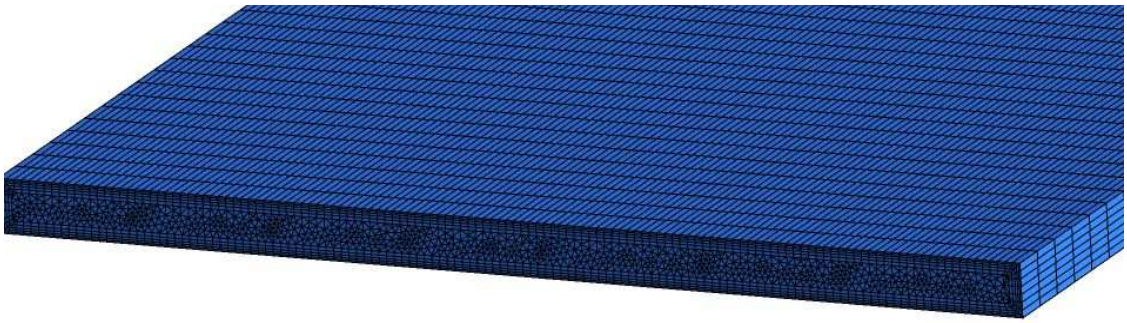

(b)

Figure 1

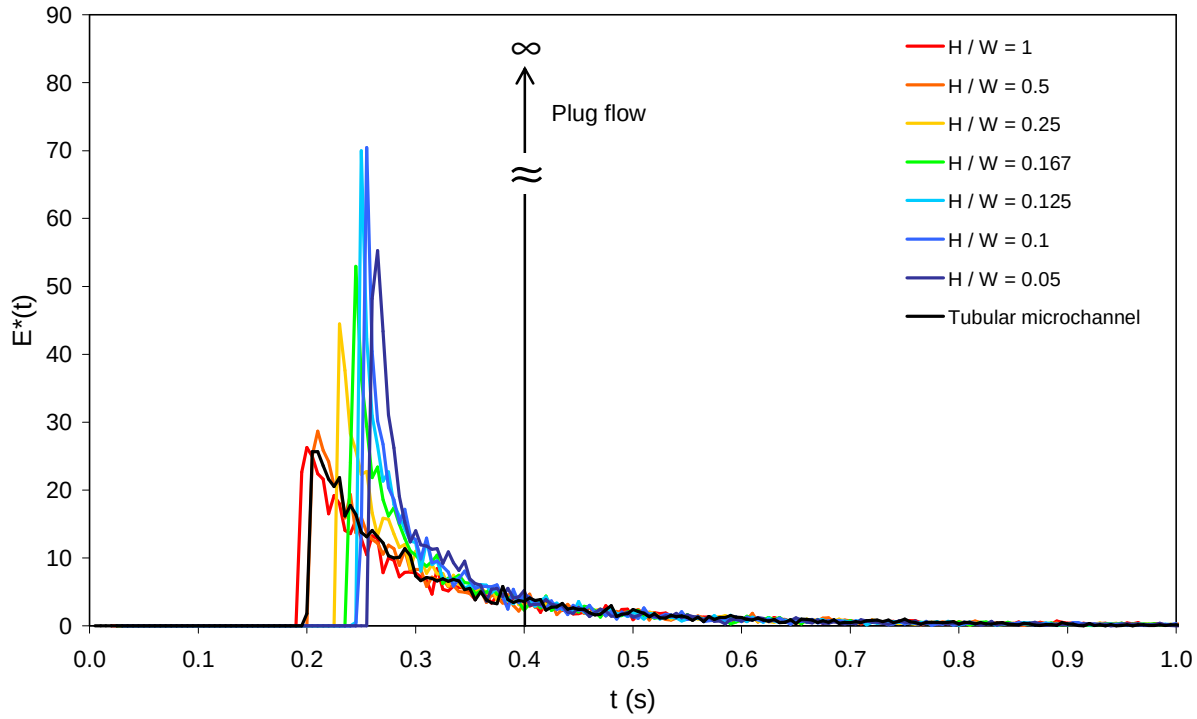
90
80
70
60
50
40
30
20
10
0
E*(t)
0.0
0.1
0.2
0.3
0.4
0.5
0.6
0.7
0.8
0.9
1.0
t (s)
∞
Plug flow
H / W = 1
H / W = 0.5
H / W = 0.25
H / W = 0.167
H / W = 0.125
H / W = 0.1
H / W = 0.05
Tubular microchannel

Figure 2

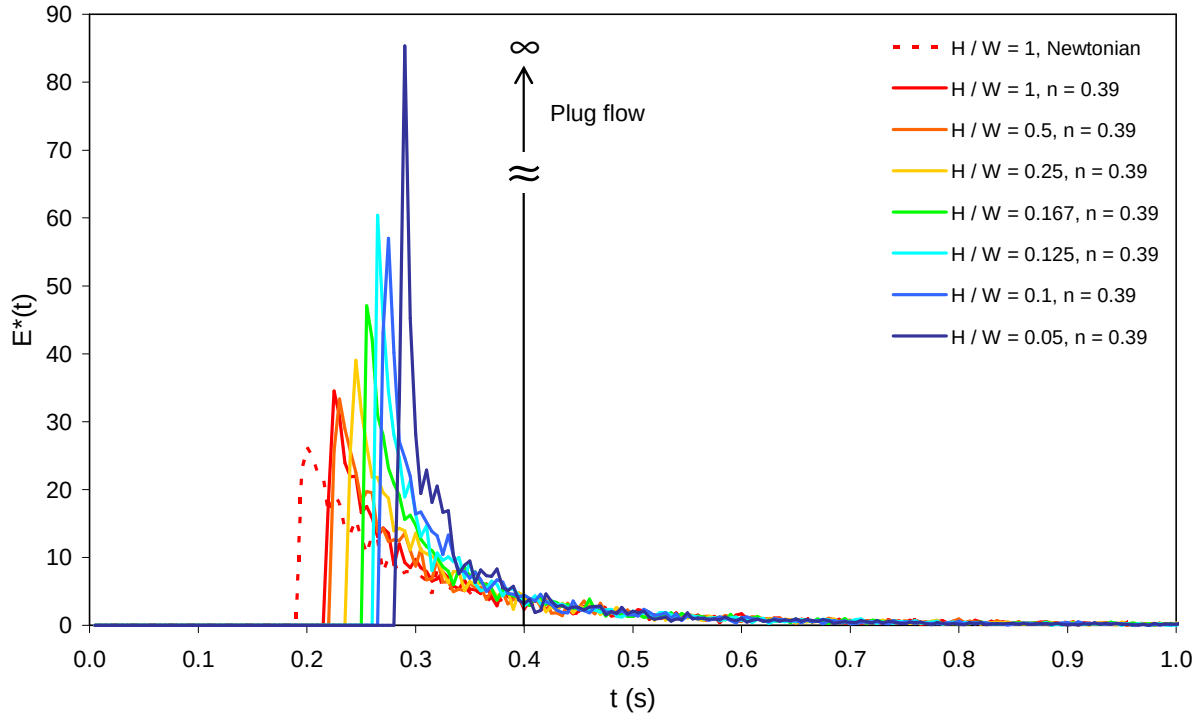
90
80
70
60
50
40
30
20
10
0
E*(t)
0.0
0.1
0.2
0.3
0.4
0.5
0.6
0.7
0.8
0.9
1.0
t (s)
∞
≈
Plug flow
H / W = 1, Newtonian
H / W = 1, n = 0.39
H / W = 0.5, n = 0.39
H / W = 0.25, n = 0.39
H / W = 0.167, n = 0.39
H / W = 0.125, n = 0.39
H / W = 0.1, n = 0.39
H / W = 0.05, n = 0.39

Figure 3

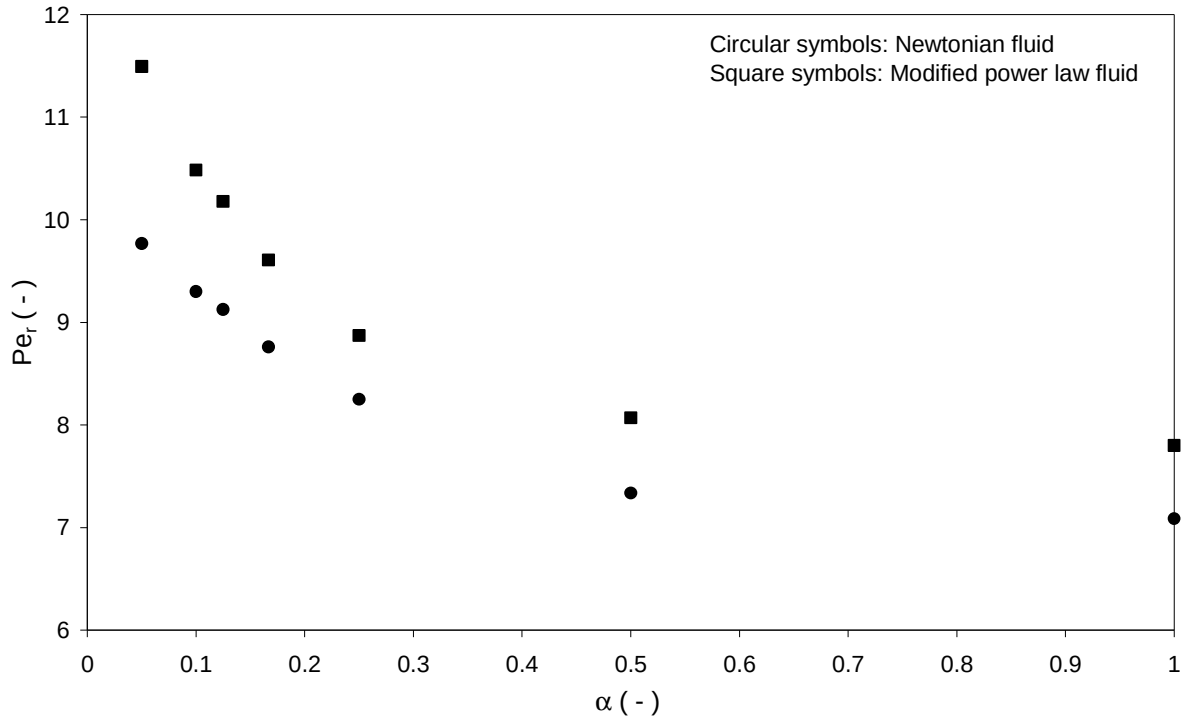
Circular symbols: Newtonian fluid
Square symbols: Modified power law fluid
Per (-)
α (-)
12
11
10
9
8
7
6
0
0.1
0.2
0.3
0.4
0.5
0.6
0.7
0.8
0.9
1

Figure 4

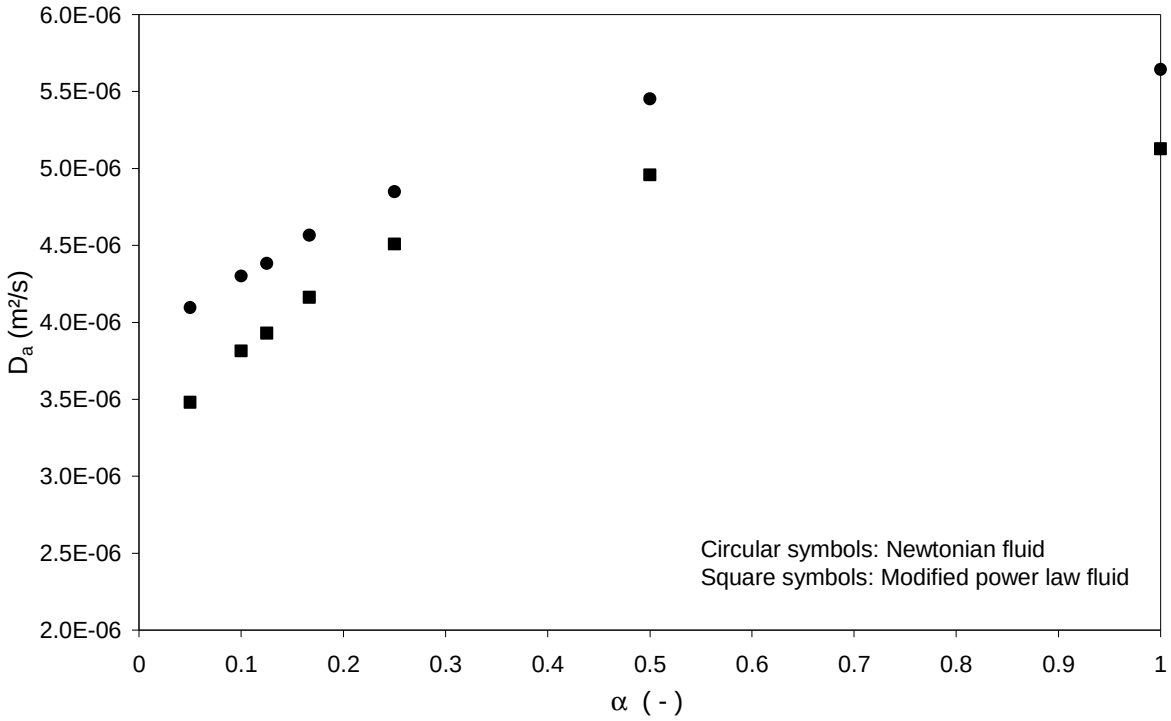
6.0E-06
5.5E-06
5.0E-06
4.5E-06
4.0E-06
3.5E-06
3.0E-06
2.5E-06
2.0E-06
D_a (m²/s)
0
0.1
0.2
0.3
0.4
0.5
0.6
0.7
0.8
0.9
1
α (-)
Circular symbols: Newtonian fluid
Square symbols: Modified power law fluid

Figure 5

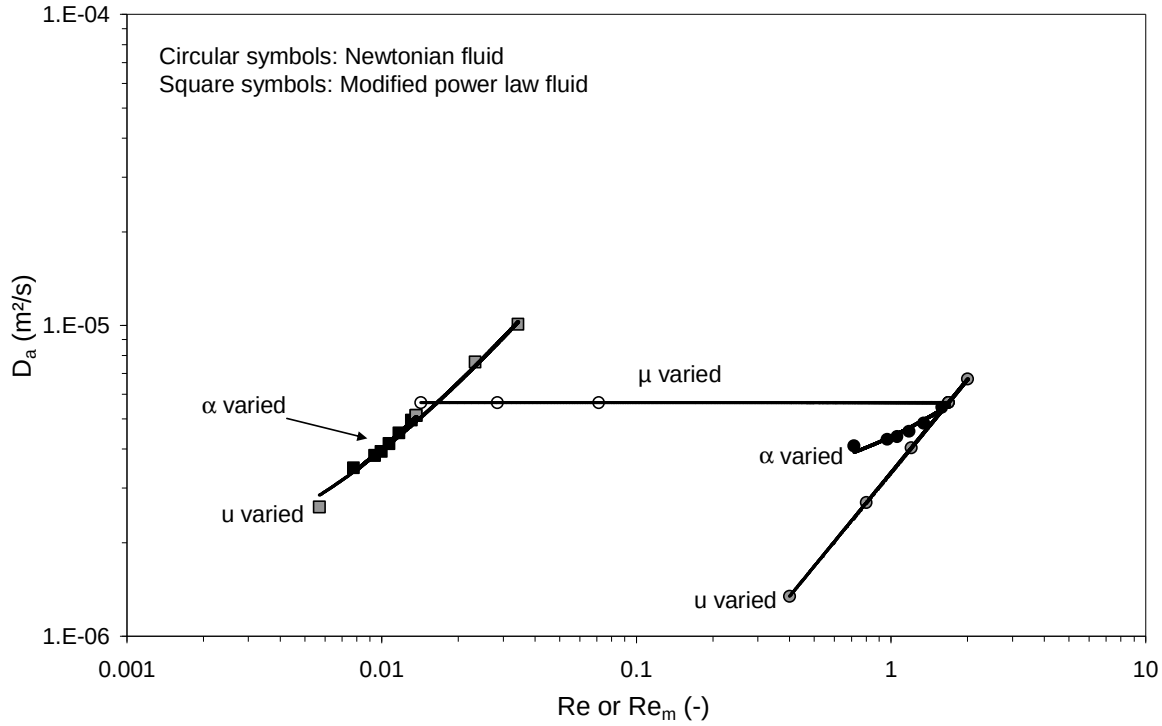
1.E-04
1.E-05
1.E-06
Da (m²/s)
Circular symbols: Newtonian fluid
Square symbols: Modified power law fluid
α varied
μ varied
α varied
u varied
u varied
0.001
0.01
0.1
1
10
Re or Rem (-)

Figure 6

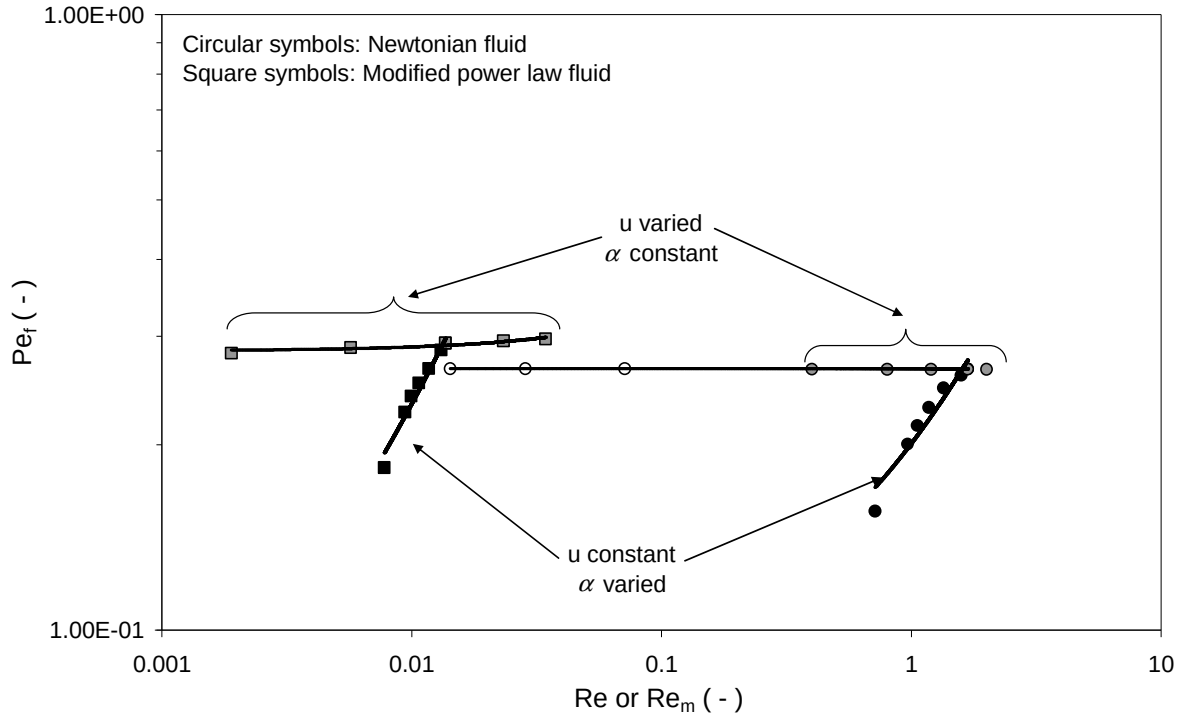
1.00E+00
Circular symbols: Newtonian fluid
Square symbols: Modified power law fluid
u varied
α constant
u constant
α varied
1.00E-01
0.001
0.01
0.1
1
10
Pe_f (-)
Re or Re_m (-)

Figure 7